



Modulating the Voltage-sensitivity of a Genetically Encoded Voltage Indicator

Arong Jung^{1,2†}, Dhanarajan Rajakumar^{1†}, Bong-June Yoon² and Bradley J. Baker^{1,3*}

¹The Center for Functional Connectomics, Korea Institute of Science and Technology, Seoul,

²College of Life Sciences and Biotechnology, Korea University, Seoul,

³Division of Bio-Medical Science and Technology, KIST School, Korea University of Science and Technology (UST), Seoul, Korea

Saturation mutagenesis was performed on a single position in the voltage-sensing domain (VSD) of a genetically encoded voltage indicator (GEVI). The VSD consists of four transmembrane helices designated S1-S4. The V220 position located near the plasma membrane/extracellular interface had previously been shown to affect the voltage range of the optical signal. Introduction of polar amino acids at this position reduced the voltage-dependent optical signal of the GEVI. Negatively charged amino acids slightly reduced the optical signal by 33 percent while positively charge amino acids at this position reduced the optical signal by 80%. Surprisingly, the range of V220D was similar to that of V220K with shifted optical responses towards negative potentials. In contrast, the V220E mutant mirrored the responses of the V220R mutation suggesting that the length of the side chain plays in role in determining the voltage range of the GEVI. Charged mutations at the 219 position all behaved similarly slightly shifting the optical response to more negative potentials. Charged mutations to the 221 position behaved erratically suggesting interactions with the plasma membrane and/or other amino acids in the VSD. Introduction of bulky amino acids at the V220 position increased the range of the optical response to include hyperpolarizing signals. Combining The V220W mutant with the R217Q mutation resulted in a probe that reduced the depolarizing signal and enhanced the hyperpolarizing signal which may lead to GEVIs that only report neuronal inhibition.

Key words: GEVI, Voltage range, Fluorescence, Voltage sensing domain

INTRODUCTION

Optical-electrophysiology is a promising technique since introducing light to biological samples can be less obtrusive and more flexible than classic electrodes. While the pixels of the optical recording device can be considered surrogate electrodes, the proper-

ties of the optical output are far different from those of electrodes. Calcium imaging with dyes or Genetically Encoded Calcium Indicators (GECIs) primarily identify activated cells firing action potentials [1]. Voltage imaging with dyes or Genetically Encoded Voltage Indicators (GEVIs) yields faster temporal resolution of action potentials as well as the optical detection of subthreshold synaptic activity and/or neuronal inhibition depending on the voltage range of the probe being used [2, 3]. This improved detection of differing types of neuronal activity combined with cell type specific expression make GEVIs a powerful tool for exploring neuronal networks.

Optimizing the voltage sensitivity of GEVIs is key to imaging

Received July 27, 2017, Revised August 19, 2017,
Accepted September 24, 2017

*To whom correspondence should be addressed.

TEL: 82-2-958-7227, FAX: 82-2-958-7219

e-mail: bradley.baker19@gmail.com

†These authors contributed equally.

neuronal activities in brain tissue [4]. For imaging individual neurons in culture, a GEVI with an optical response over a broad voltage range is desirable for observing the differing types of membrane potential changes [5]. However, when imaging a large population of cells in slice or in vivo, a broad voltage range could be a disadvantage. One problem is that the total fluorescence change of a probe is diluted over these different neuronal activities. Since the amount of functional probe is limited to the plasma membrane, signal to noise ratios of GEVIs are much lower than GECIs. The total amount of fluorescent probe is lower. In addition, poor trafficking to the plasma membrane creates an internal, non-responsive fluorescence as well. Focusing the fluorescence change to a more narrow voltage range would help detect the optical signal. Another consequence of a broad voltage range for a GEVI when imaging populations of cells is that the membrane potential of neighboring cells may not be synchronized. Most GEVIs exhibit opposite fluorescent signals for hyperpolarization of the plasma membrane versus depolarization of the plasma membrane [6-8]. When imaging a population of cells, more than one neuron will contribute fluorescence to a pixel. The relatively small increase of the fluorescence from a hyperpolarizing event can be masked by the depolarization of a neighboring cell. In these cases, it might prove helpful to modify the voltage-sensitivity of a GEVI to optimize the optical signal for a specific type of neuronal activity.

There are multiple ways to modify the voltage range of a GEVI [6-9]. Changing the number of amino acids (linker length) between the voltage sensing domain (VSD) and the fluorescent protein shifted the $V_{1/2}$ (the voltage at which half of the total fluorescence change occurs) of Bongwoori to near zero mV [10]. Mutations to the VSD can also change the $V_{1/2}$. The classic example is VSFP2.1 which introduced the R217Q mutation to the VSD of the probe [6]. These altered voltage ranges are usually a consequence of moving the $V_{1/2}$ to more negative or positive potentials. Ideally one would like to also limit the entire voltage range of a GEVI thereby focusing the fluorescent change. The fourth transmembrane helix segment (S4) of the VSD was found to have the most profound effects on the voltage sensitivity [10]. A V220T mutation in the VSD was found to shift the $V_{1/2}$ by increasing the voltage range of the GEVI, CC1. CC1 is an ArcLight-type probe utilizing the VSD of the voltage-sensing phosphatase from *Ciona intestinalis* [11] that requires a strong depolarization of the plasma membrane to induce an optical signal [10, 12]. In an attempt to modify the voltage range, saturation mutagenesis of the V220 position was performed. Two interesting results were observed. The first was that the size of the R-group for charged amino acids at that position affected the voltage-dependent signal. The second was that a tryptophan mutant (R217Q/V220W) inhibited the voltage-

dependent signal at distinct voltages. The bulky side chain of tryptophan may impede the movement of the S4 transmembrane segment. Manipulation of that inhibition to limit the movement of the VSD to specific voltage ranges could lead to GEVIs that respond to distinctive neuronal activities, e.g. inhibition.

MATERIALS AND METHODS

Construct design

The V220 position of the S4 domain in the GEVI, CC1 [10], was mutated by 2-step PCR reactions. CC1 constructs were changed to the 20 amino acid combinations each, using primers (Cosmogentech) listed in supplementary Table 1. PCR was used to introduce a 5' Eco RV site and a 3' Xho I site for the introduction of SE 227D resulting in the acid composition to be RYR at the fusion site of the fluorescent protein with pcDNA 3.1 vector. All constructs were verified by DNA sequencing (Cosmogentech, Republic of Korea).

Transient expression of GEVIs in mammalian cells

HEK293 cells were maintained in Dulbecco's Modified Eagle Medium (High Glucose DMEM; Gibco, USA) supplemented with

Table 1. Physical characteristics of the V220X mutants

Constructs (V220X)	$\Delta F/F_{\max}$ (200 mV)	Weighted τ on	Weighted τ off
CC1 (WT)	15±1.1	35±15.2	48±11.8
V220G	7±0.5	21±4.8	9±0.6
V220A	9±1.8	23±7.1	21±4.3
V220L	16±0.6	37±0.1	22±2.0
V220I	10±0.9	>100	>100
V220M	2±0.3		
V220C	8±0.3	26±2.0	25±3.7
V220P	7±0.5	32±7.9	69±46.2
V220F	14±0.5	14±1.5	10±1.2
V220W	9±0.4	10±0.6	6±0.2*
V220Y	8±0.7	9±0.4*	6±0.9
V220Q	1±0.1		
V220N	1±0.1		
V220S	5±0.9	45±12.3	10±1.2
V220T	11±0.5	28±2.6	20±2.3
V220H	2±0.4		
V220D	10±1.0	15±3.2	94±8.6
V220E	12±1.0	23±3.6	25±1.9
V220R	3±0.2	59±10.0	12±0.6
V220K	2±0.2		

Constructs list the substitution to the V220 position. CC1 (WT) is V220. The $\Delta F/F_{\max}$ is the signal size for a 200 mV depolarization of the plasma membrane. The weighted on and off time constants are described in materials and methods. The time constants depicted with an asterisk exhibit single exponential fits. All other time constants were better fit with a double exponential function.

10% (v/v) fetal bovine serum (FBS; Invitrogen, USA) and 0.1X of Glutamax solution (Invitrogen). For transient transfection, HEK293 cells were dissociated with 0.25% of trypsin-EDTA (Invitrogen) and then seeded onto #0 coverslips coated with poly-D-lysine (Sigma). Transient protein expression in HEK cells was done by using Lipofectamine 2000 (Invitrogen) according to manufacturer instructions (Invitrogen).

Electrophysiology

Transfected HEK293 cells were patched in the whole cell voltage clamp mode at 34°C and perfused with bath solution containing 150 mM NaCl, 4 mM KCl, 2 mM CaCl₂, 1 mM MgCl₂, 5 mM D-Glucose, and 5 mM HEPES (pH 7.4). 3-5 MΩ glass patch pipettes (World Precision Instruments, FL) were pulled by a P-97 micropipette puller (Sutter Instrument Company). The internal pipette solution contained 120 mM K-aspartate, 4 mM NaCl, 4 mM MgCl₂, 1mM CaCl₂, 10 mM EGTA, 3 mM Na₂ATP and 5 mM HEPES, (pH 7.2). Whole-cell voltage-clamp recordings of transfected HEK293 cells were done using an EPC10 amplifier (HEKA). Voltage steps are as indicated in the figures and usually consisted of a 50 or 100 mV hyperpolarization of the plasma membrane followed by a 50 mV, 100 mV, 150 mV, and 200 mV depolarizations for 200 ms of the plasma membrane.

Arc Lamp and wide field imaging

During the patch clamp experiments the cells were imaged on an IX71 microscope with a 60× 1.35-numerical aperture (NA) oil-immersion lens (Olympus). Fluorescence excitation was delivered using a 75 W Xenon Arc lamp (Cairn). The filter set used was that reported for ArcLight [7]. The excitation filter was FF02-472/30 (Semrock). The emission filter was FF01-496/LP (Semrock). The dichroic was FF495-Di03 (Semrock). The objective C-mount image was de-magnified by an Optem zoom system A45699 (Qioptiq LINOS, Inc., Fairport, NY) and projected onto the e2v CCD39 chip of NeuroCCD-SM 80 pixel x 80 pixel camera (RedShirtImaging). The imaging apparatus was mounted on a Vibraplane Bench Top vibration isolation platform (Minus K Technology). The mechanical shutter in the incident light patch was mounted on a separate table. Images were recorded at a frame rate of 1kfps. The excitation light was 1 mW/mm².

Optical signal analysis

Optical signal recordings were analyzed using Neuroplex (Red-shirtImaging), Excel (Microsoft), and Origin 8.6 (OriginLab). The fluorescent traces for constructs expressed in HEK cells were averages of 16 trials. Regions of interests were identified by subtracting the steady-state fluorescence of frames during the holding

potential from the frames during the 200 mV depolarization [13]. For ΔF/F measurements, F was defined as the fluorescence average of the first five frames of the recording. For the kinetics, the optical traces were fitted to a double exponential decay:

$y=y_0+A_1e^{-(t-t_0)/\tau_1}+A_2e^{-(t-t_0)/\tau_2}$ where t is time in milliseconds, and a single exponential decay:

$y=y_0+A_1e^{-(t-t_0)/\tau_1}$ where t is time in milliseconds.

To compare the optical responses that were better fitted to a single exponential decay to those better fitted by a double exponential decay, a weighted tau was calculated as the sum of τ₁ multiplied by the relative amplitude, A₁, plus τ₂ multiplied by the relative amplitude, A₂, as defined by the following formula:

$$\tau_w = \tau_1(A_1/(A_1+A_2)) + \tau_2(A_2/(A_1+A_2))$$

The voltage-sensitivity was determined by initially fitting individual cell responses to the Boltzmann equation:

$$y=(A_1-A_2)/(1+e^{-(x-x_0)/dx})+A_2$$

where y is -ΔF/F, and x is membrane potential in mV. A₁ is the minimum value defined as zero, and A₂ is the maximum value defined as one. x₀ is the membrane potential in mV at half maximal ΔF/F, and dx is the slope at x₀. All traces were normalized such that A₁=0 and A₂=1. The trials for each construct were then averaged and refit.

RESULTS

The V220T mutation shallows the slope of the voltage-range for the optical signal of the GEVI, CC1

CC1 utilizes the VSD of the voltage-sensing phosphatase from *Ciona intestinalis* which is fused to a pH sensitive fluorescent protein (FP), supercliptic pHlorin [7, 10, 14, 15]. The S4 transmembrane segment has positively charged amino acids every third residue (Fig. 1A). This pattern is interrupted by a valine at the amino acid 220 position. In a previous report, changes to the V220 position resulted in a shift in the voltage-sensitivity of the probe [10]. The V220R mutation shifted the voltage-sensitivity to more positive potentials. The V220T mutation shifted the voltage-sensitivity to more negative potentials. Fig. 1A reproduces these result showing the optical traces during whole cell voltage clamp of HEK293 cells expressing CC1, the V220R mutant, or the V220T mutant.

The Boltzman fit of the fluorescence change versus membrane potential suggests that the V220T changes the V_{1/2} by altering the slope of the response compared to that of CC1 (Fig. 1A). These fits are a bit tenuous due to the fact that it is difficult to depolarize HEK293 cells beyond +130 mV to experimentally determine the maximum signal size. However, the optical traces also suggest a change in the slope. Both the CC1 construct and the V220T

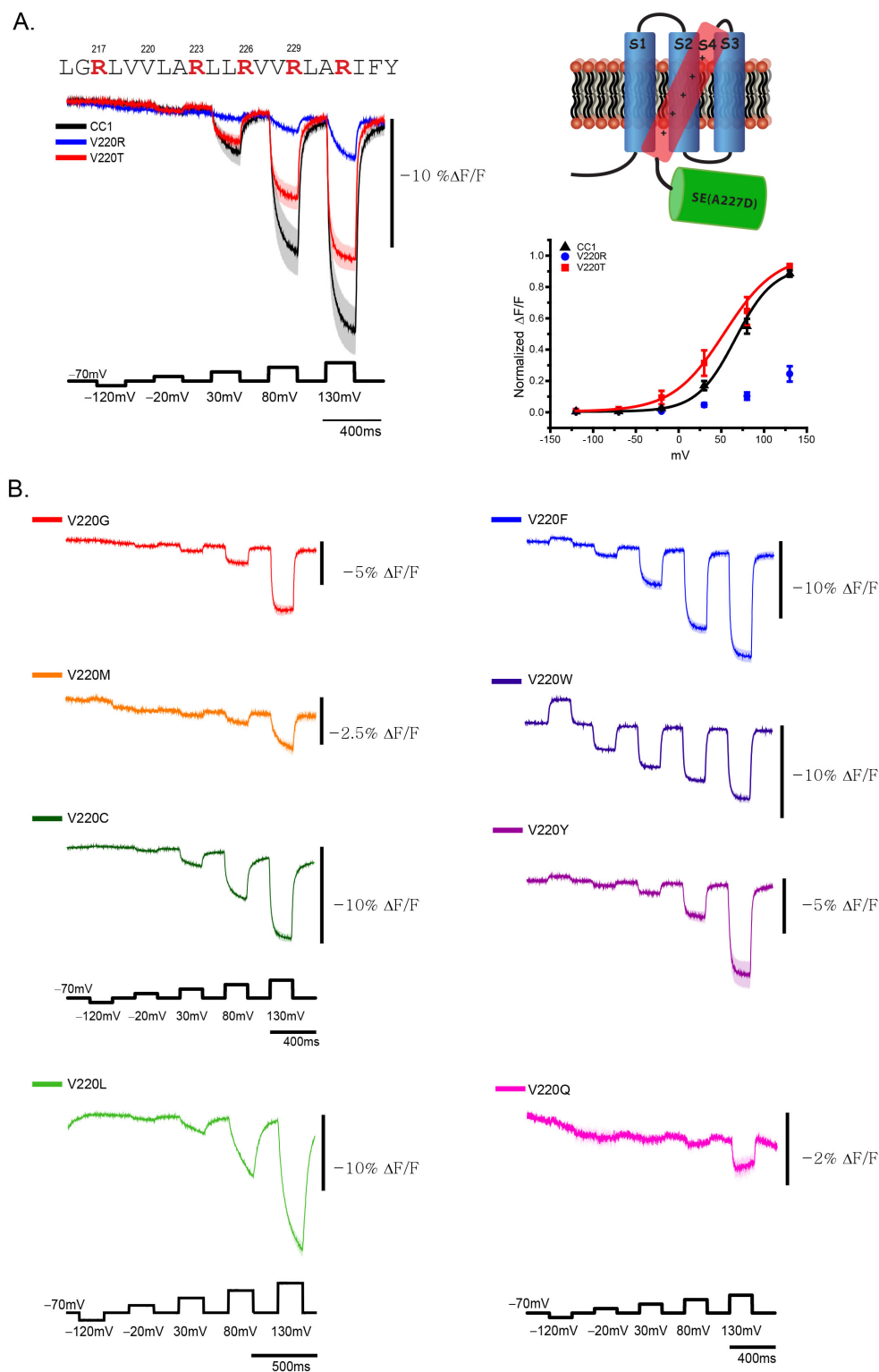


Fig. 1. Mutations to the V220 position in the S4 transmembrane helix affects the voltage range of the GEVI. A. Comparison of the V220R and V220T mutants. The protein sequence of the S4 transmembrane helix of CC1 shows the classic RXXR motif. The schematic of the GEVI, CC1 with the voltage-sensing domain in the plasma membrane and the fluorescent protein, super ecliptic pHlorin with the A227D mutation[29] depicted in green in the cytoplasm. Positively charged residues are red. Optical traces are from whole-cell clamped HEK 293 cells expressing CC1 (black), V220R (blue), or V220T (red) subjected to a series of voltage steps. The dark lines are the average of at least 4 cells. Shaded area is the standard error of the mean. Right graph is a Boltzman plot of the normalized fluorescence change. The V220R mutant does not have enough data points for a reliable fit. B. Representative examples of mutations to the V220 position. See table one for complete list. Command voltage pulses are depicted in black.

mutant give similar optical signals for the 100 mV depolarization from a holding potential of -70 mV to +30 mV. Increasing the depolarization step to 150 mV resulted in a larger change for the CC1 construct versus the V220T mutant which is indicative of an altered slope. Saturation mutagenesis was therefore performed at the V220 position in an effort to better tune the voltage response.

The amino acid side chain size and composition affects the voltage sensitivity of CC1

The crystal structure of the voltage sensing domain suggests that the V220 position resides in the lipid bilayer near the plasma membrane/extra-cellular interface [16]. Of the 19 substitutions tested, only the V220L mutant exhibited a similar signal size for a 200 mV depolarization step when compared to CC1 (Table 1). This conservative amino acid change results in the addition of a methyl group to the side chain suggesting that other aliphatic amino acids would be well tolerated. That was not the case as the V220G, V220A, V220I, V220P mutants all reduced the optical signal by roughly 50% (Fig. 1B). Surprisingly, the V220M mutant reduced the signal eight-fold to 2% $\Delta F/F/200$ mV which could be due to an intolerance of the sulfur atom in the methionine side chain. However, the V220C mutation only reduced the optical signal by 50% (8% $\Delta F/F/200$ mV).

Some of these mutant GEVIs as well as the CC1 construct exhibit slow responses that do not plateau during the voltage command pulse. A consequence of this slow response is the under representation of the maximal fluorescence change. A slow optical signal can be overcome if the magnitude of the response is large. ArcLight is a prototypical example. ArcLight has an on tau of over 10 ms but gives a 40% $\Delta F/F/100$ mV [7, 17]. This large signal size can overcome the slow speed of the response enabling the optical resolution of action potentials firing at 35 Hz [12]. Unfortunately, none of the V220 mutants give very large signals but do provide insights into manipulating the voltage range.

Amino acids with a bulky side chain all altered the voltage range of the GEVI. V220F shifted the $V_{1/2}$ from about +100 mV to +50 mV. The V220W exhibited the largest shift towards negative potentials having a $V_{1/2}$ of -40 mV which can be seen by the increase in fluorescence upon hyperpolarization of the plasma membrane (Fig. 1B and Table 1). The V220Y mutant was also able to report the hyperpolarization of the plasma membrane. However, the signal remains small until the plasma membrane is depolarized by 150 mV making it difficult to fit to a Blotzman plot.

The polar, uncharged amino acid substitutions in general were very deleterious to the optical signal. V220N, V220Q, and V220H all had optical signals of 2% $\Delta F/F/200$ mV or less (Fig. 1C and Table 1). The V220S mutant was slightly better with a 5% $\Delta F/F/200$

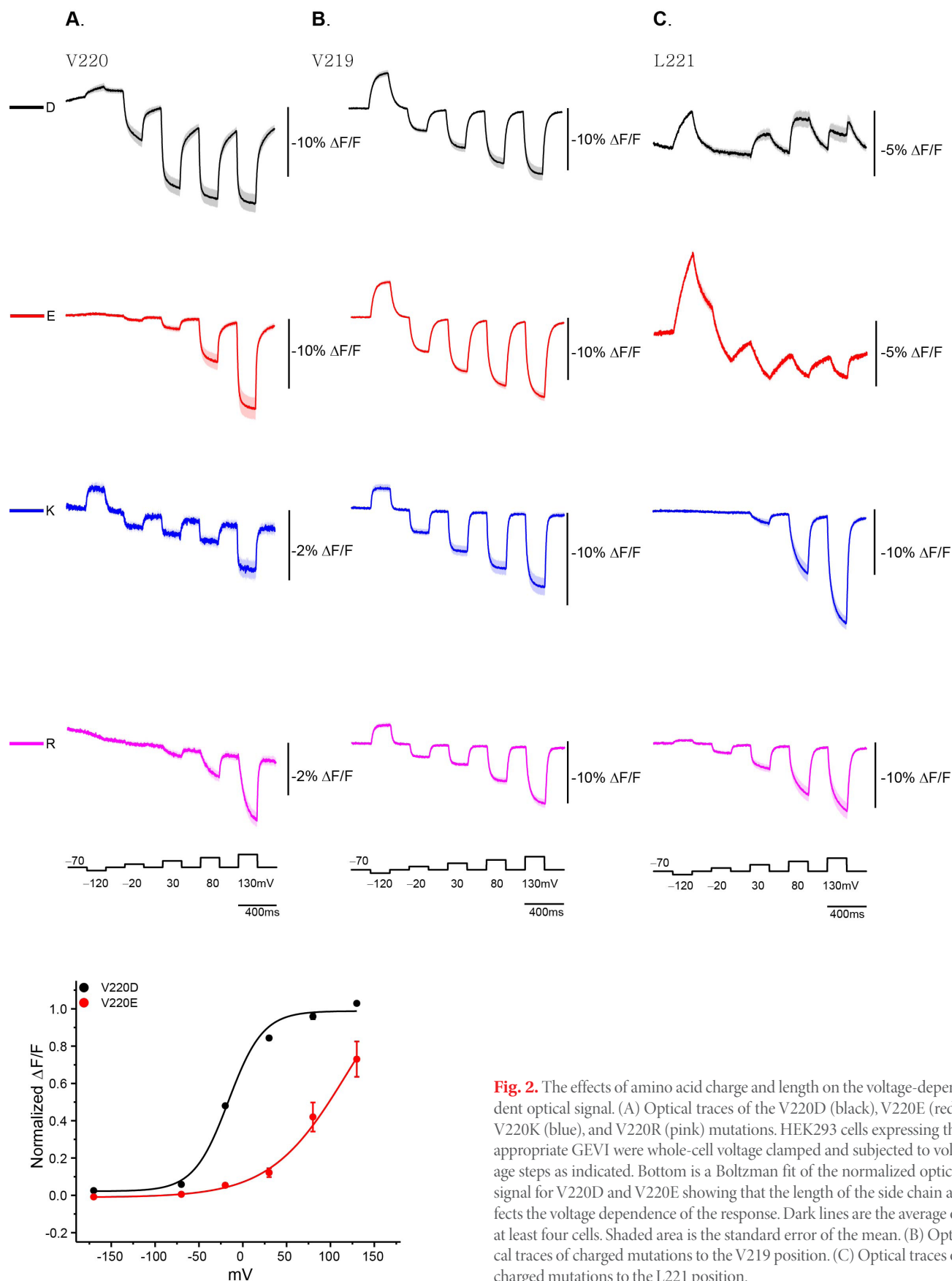
mV signal. Extending the side chain by a methyl group doubled the optical signal with the V220T mutant having an 11% $\Delta F/F/200$ mV signal. These results suggested that the length as well as the polarity of the side chain affected the voltage-dependent optical signal.

The size of the amino acid side chain affecting the optical signal could also be seen for V220 substitutions containing a charged residue. Substitutions with a positively charged amino acid were as deleterious as the polar substitutions mentioned above. The V220R mutant had a signal of 3% $\Delta F/F/200$ mV, and the V220K construct was even worse exhibiting 1% $\Delta F/F/200$ mV. Surprisingly, the voltage range of V220K was different from V220R. The V220R mutant voltage range was similar to the original CC1 construct (Fig. 2A). Indeed, the V220R mutant might be slightly shifted to more positive potentials since the 200 mV depolarization more than doubles the signal compared to the 150 mV depolarization. The optical signal over the same voltages for CC1 shows a more modest increase (Fig. 1). V220K on the other hand has extended the voltage range of the optical signal to more negative potentials. The V220K despite its small signal size can optically detect a hyperpolarization of the plasma membrane.

The V220 position was more tolerant of negatively charged amino acids. V220D and V220E both had signals of 10% $\Delta F/F/200$ mV. However, these probes exhibited different voltage ranges as well (Fig. 2A). V220E mirrored the CC1 and the V220R voltage ranges. The V220D mutant clearly shifted the voltage range to more negative potentials. For both positive and negative substitutions at the V220 position, the length of the side chain affected the voltage range while the polarity of the charge affected the signal size. The V219 position tolerated both positive and negative amino acid substitutions with all four mutants exhibiting similar voltage ranges (Fig. 2B). All V219 charged substitutions shifted the optical signal to more negative potentials. The L221 position was more tolerant of positive amino acid substitutions giving at least a 10% $\Delta F/F/200$ mV depolarization pulse (Fig. 2C). In contrast to the V220 position, introduction of negatively charged amino acids at this position reduced the signal to 5% $\Delta F/F/200$ mV and altered the polarity of the optical signal for the L221D mutant. The voltage range was also reversed for the positively charged substitutions. The L221K did not show a hyperpolarizing signal while the L221R did. The odd behavior of the negative charges in the L221 position could reflect interactions with other parts of the VSD and/or the plasma membrane.

Combining S4 mutations to further tune the voltage range of the GEVI

One driving force in the development of GEVIs is to make a



probe that is biased towards reporting neuronal inhibition. This effort requires shifting the voltage response of the GEVI to very negative potentials. One well documented mutant that shifts the voltage range from +100 mV (the $V_{1/2}$ for CC1) to -50 mV is the R217Q mutation in the S4 transmembrane segment of the VSD [6].

To further shift the $V_{1/2}$ to membrane potentials that occur during neuronal inhibition, several V220 mutants were combined with the R217Q mutation.

The R217Q mutation was unable to shift the voltage response to more negative potentials when the V220 position contained a

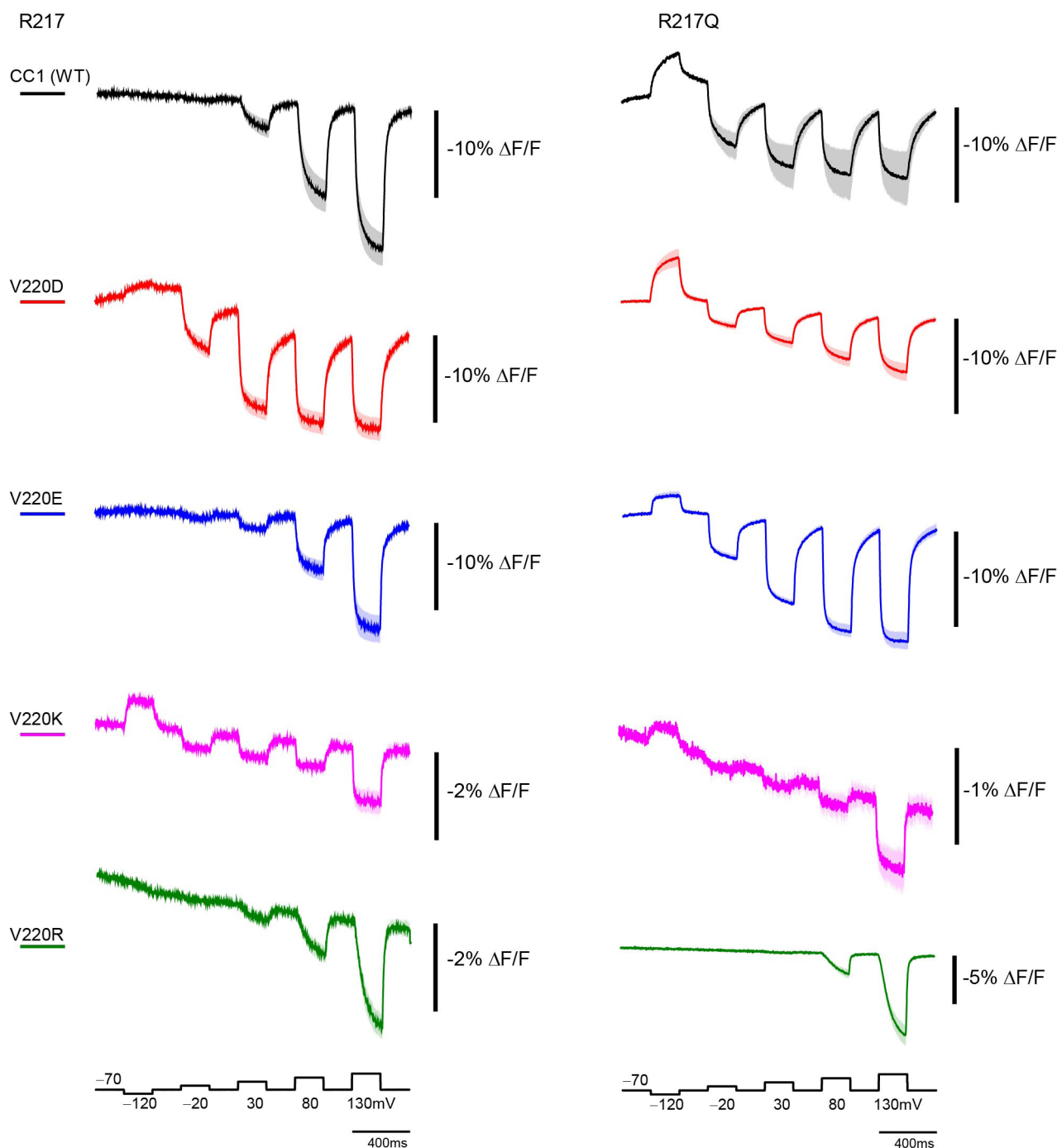


Fig. 3. Combining the charged V220 mutants with the R217Q mutation. The optical traces of the charged V220 mutants in the presence of the R217 wildtype sequence (same as in Fig. 2 shown here for ease of comparison) are on the left. On the right are the same charged mutants in the presence of the R217Q mutation. Only the negatively charged V220 mutants show an increase in the optical signal during the hyperpolarizing voltage step.

positively charged amino acid (Fig. 3). The fluorescence response during the hyperpolarizing pulse for V220K and V220R does not improve when the R217Q mutation is added. An increase in the fluorescence response can be seen for the V220D and V220E

mutants in the presence of the R217Q substitution. In addition to shifting the voltage sensitivity, the R217Q mutation lowered the signal size of the optical signal for depolarization steps of the plasma membrane. The R217Q/V220D mutant exhibited a signal that

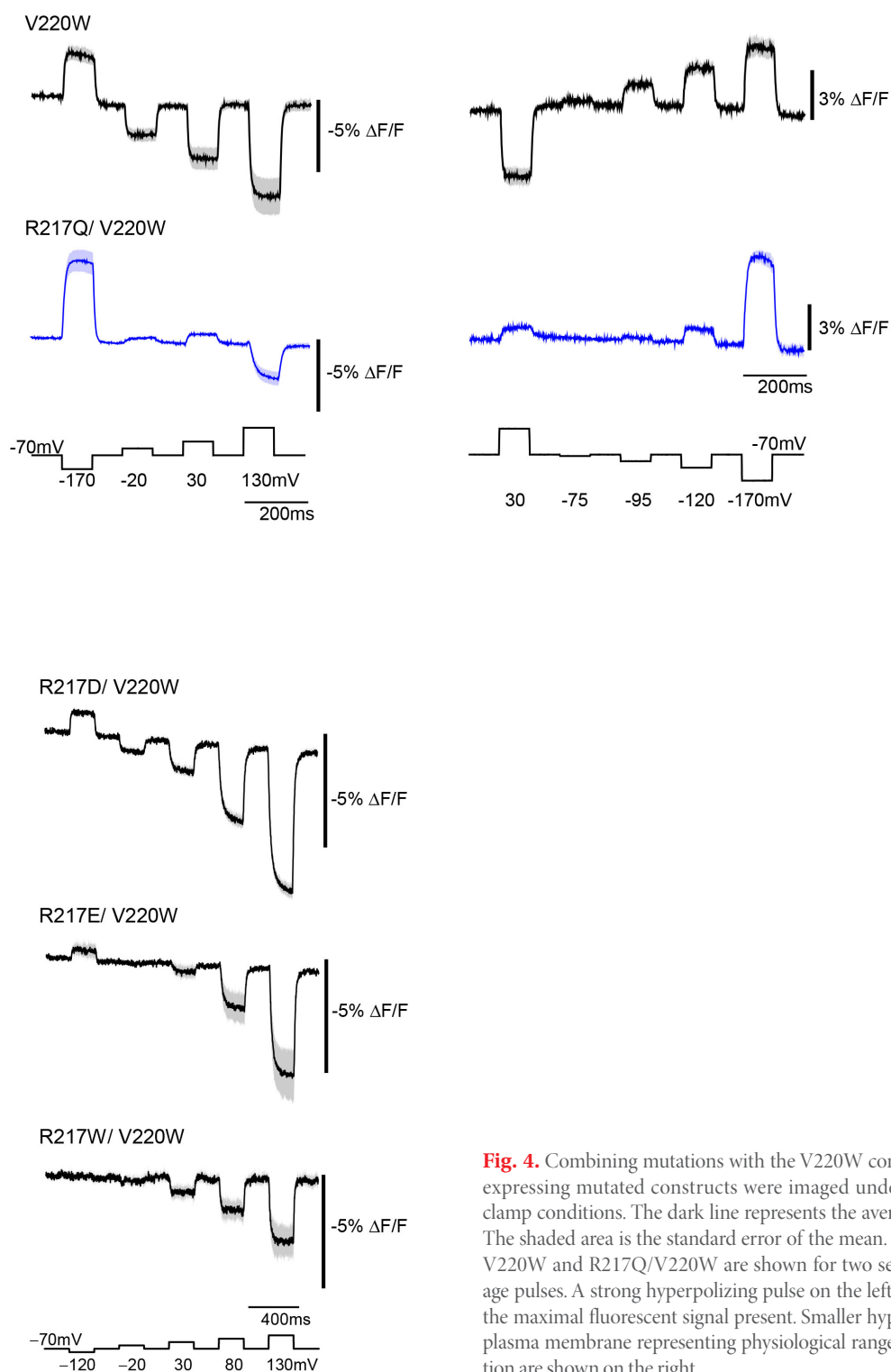


Fig. 4. Combining mutations with the V220W construct. HEK293 cells expressing mutated constructs were imaged under whole-cell voltage clamp conditions. The dark line represents the average of at least 4 cells. The shaded area is the standard error of the mean. Optical responses for V220W and R217Q/V220W are shown for two sets of command voltage pulses. A strong hyperpolarizing pulse on the left was done to observe the maximal fluorescent signal present. Smaller hyperpolarization of the plasma membrane representing physiological ranges of neuronal inhibition are shown on the right.

is half the magnitude of the V220D construct for a 200 mV depolarization (5% $\Delta F/F$ versus 10% $\Delta F/F$). However, the R217Q/V220E mutant maintained the signal size for a 200 mV depolarization compared to the V220E construct. Neither the R217Q/V220R nor the R217Q/V220K mutants showed a significant change in the voltage range when compared to the V220R or V220K mutants. Interestingly, the R217Q/V220R tripled the size of the optical signal for a 200 mV depolarization when compared to the V220R mutant.

Combination of the V220W mutant with other mutations at the R217 position resulted in some interesting phenotypes (Fig. 4). The V220W mutant elongates the voltage response of the probe over a very large range. When combined with the R217Q mutation (R217Q/V220W), the optical response was increased for the hyperpolarizing pulse and decreased for the depolarizing pulses. Surprisingly, the polarity of the fluorescence change for the 50 mV depolarization step and the 100 mV depolarization step was reversed. While this unexpected behavior is difficult to explain, this pattern of activity is better suited for imaging neuronal inhibition. The R217Q/V220W has a smaller signal for the 100 mV depolarization step and a small but observable signal when the plasma membrane is hyperpolarized by 15 mV.

Further investigation of the R217 position in combination with the V220W mutation suggested that tryptophan can restrict the voltage range of the optical signal. The crystal structure of the up-state of the VSD from the voltage-gated phosphatase was achieved by mutating the R217 position to glutamic acid [16]. That mutation shifted the voltage response to more negative potentials enabling the structure of the up-state to be solved. The R217E/V220W had a small hyperpolarizing signal and no detectable signal for a 50 mV depolarization of the plasma membrane. The R217D/V220W construct had a reduced hyperpolarizing signal. Introduction of tryptophan at the 217 position (R217W/V220W) created a probe that only responded to a 100 mV or greater depolarization of the plasma membrane, an ideal probe for action potentials if the signal size was larger.

DISCUSSION

It may be possible to manipulate the voltage range of a GEVI to optically image specific types of neuronal activity. Mutagenesis to the VSD or the linker sequence connecting the FP to the VSD can alter the voltage range. Unfortunately, there are no clear rules. The voltage tuning of a GEVI is an empirical process. The V220 position had been shown to affect the voltage range of the optical response [10]. Saturation mutagenesis of that position revealed that side chain length and polarity affect the voltage range, signal

size, and speed of the optical response. The faster responses were achieved by replacement with bulky side chain amino acids which improved the speed from 35 ms to around 10 ms (Table 1).

In addition to optically reporting changes in plasma membrane potentials, GEVIs also offer insights into the functioning of the VSD complementary to gating currents [18-20], state-dependent accessibility of an amino acid [21], or site-directed fluorescently labeling [22]. We and others have shown that the movement of the S4 transmembrane domain is responsible for the voltage-dependent optical signal [23, 24]. Replacing V220 with a positively charged amino acid reduced the signal size by a factor of 5 while negatively charged residues only reduced the signal by 33%. Yet, the voltage range was more affected by the size of the side chain than the charge (Fig. 2). This suggests the potential hypothesis that a slight alteration in the location of a charged molecule in a hydrophobic environment may affect the position of the S4 transmembrane segment thereby altering the voltage sensitivity. When the hydrophobic length of the transmembrane helix is mismatched to the thickness of the lipid bilayer, the protein helix may tilt and/or the thickness of the membrane may thin (or thicken depending on the mismatch) [25]. It may be that the extra carbon molecule in the glutamic acid residue enables the charged portion of the molecule to exit the hydrophobic region of the lipid bilayer resulting in a probe that more resembles the wildtype voltage response pattern.

GEVIs may also optically disclose protein/membrane interactions. The fact that the charged residues at the V220 position give smaller signals may be indicative of an interaction with the lipid head groups of the plasma membrane. Positively charged residues interacting with the negatively charged lipid head groups could create a stronger energy barrier that reduces the movement of S4. Support for this hypothesis comes from the fact that moving the charged residue up a single amino acid to the V219 position had virtually no effect on the voltage-dependent optical signal suggesting that the charged residues are clear of plasma membrane interactions.

The R217Q mutation also suggests that the charged residues at the V220 position are interacting with the lipid head groups of the plasma membrane. The R217Q mutation has been employed by several GEVIs to shift the voltage-response to more physiological ranges [6, 7, 10, 26]. When combined with the R217Q mutation, only the V220 positively charged amino acids showed no shift towards negative potentials in the optical response of the probe (Fig. 3). When negatively charged amino acids are at the V220 position, an increase in the hyperpolarizing signal is seen. It is known that the R217E mutant alters the position of the S4 transmembrane segment at 0 mV compared to the wildtype protein from the crystal structure [16]. It seems reasonable that these mutations may

also affect the position of S4 at other membrane potentials. The R217Q mutant may alter the position of the S4 helix at -70 mV (holding potential) enabling the probe to respond to more negative potentials. However, the double mutants (R217Q/V220R or R217Q/V220K), may interact with the lipid head groups in such a manner to negate the R217Q effect. The crystal structures of these mutants should answer several of these questions.

Tryptophan has the ability to decrease the optical signal for specific voltage ranges. Regardless of the mechanism behind these differing responses, the tryptophan substitution mutants exhibit some interesting and potentially useful characteristics (Fig. 4). The V220W mutant's optical signal is spread out over at least a 250 mV range. In an effort to shift to even more negative potentials, The V220W mutation was combined with the R217Q substitution. Excitingly, this probe reduces the optical signal seen for depolarization of the plasma membrane while increasing the hyperpolarizing optical signal (Fig. 4). The bulky side chain of the tryptophan residue makes a natural anchor for transmembrane helices [27, 28]. Another possibility is that this bulky side chain is interacting with other amino acids in the voltage sensing domain creating steric hindrance for the movement of the S4 segment when the plasma membrane potential changes. Whatever the mechanism, tryptophan substitutions could potentially inhibit the movement of the S4 transmembrane segment in such a way that the probe will only respond to neuronal inhibition. For instance, a tryptophan residue that resides under the lipid head group of the outer leaflet of the plasma membrane could inhibit the outer motion of S4 during depolarization of the plasma membrane. Such a probe would still be able to respond to hyperpolarization resulting in a GEVI that would optically report only neuronal inhibition.

ACKNOWLEDGEMENTS

This study was funded by the Korea Institute of Science and Technology (KIST) grants 2E26190 and 2E26170. Research in this report was also supported by the National Institute Of Neurological Disorders And Stroke of the National Institutes of Health under Award Number U01NS099691. The content is solely the responsibility of the authors and does not necessarily represent the official views of the National Institutes of Health.

REFERENCES

- Berger T, Borgdorff A, Crochet S, Neubauer FB, Lefort S, Fauvet B, Ferezou I, Carleton A, Lüscher HR, Petersen CC (2007) Combined voltage and calcium epifluorescence imaging in vitro and in vivo reveals subthreshold and suprathreshold dynamics of mouse barrel cortex. *J Neurophysiol* 97:3751-3762.
- Storace DA, Braubach OR, Jin L, Cohen LB, Sung U (2015) Monitoring brain activity with protein voltage and calcium sensors. *Sci Rep* 5:10212.
- Empson RM, Goulton C, Scholtz D, Gallero-Salas Y, Zeng H, Knöpfel T (2015) Validation of optical voltage reporting by the genetically encoded voltage indicator VSFP-butterfly from cortical layer 2/3 pyramidal neurons in mouse brain slices. *Physiol Rep* 3:e12468.
- Nakajima R, Jung A, Yoon BJ, Baker BJ (2016) Optogenetic monitoring of synaptic activity with genetically encoded voltage indicators. *Front Synaptic Neurosci* 8:22.
- Storace D, Sepehri Rad M, Kang B, Cohen LB, Hughes T, Baker BJ (2016) Toward better genetically encoded sensors of membrane potential. *Trends Neurosci* 39:277-289.
- Dimitrov D, He Y, Mutoh H, Baker BJ, Cohen L, Akemann W, Knöpfel T (2007) Engineering and characterization of an enhanced fluorescent protein voltage sensor. *PLoS One* 2:e440.
- Jin L, Han Z, Platasa J, Woollorton JR, Cohen LB, Pieribone VA (2012) Single action potentials and subthreshold electrical events imaged in neurons with a fluorescent protein voltage probe. *Neuron* 75:779-785.
- Platasa J, Vasan G, Yang A, Pieribone VA (2017) Directed evolution of key residues in fluorescent protein inverses the polarity of voltage sensitivity in the genetically encoded indicator ArcLight. *ACS Chem Neurosci* 8:513-523.
- Jung A, Garcia JE, Kim E, Yoon BJ, Baker BJ (2015) Linker length and fusion site composition improve the optical signal of genetically encoded fluorescent voltage sensors. *Neurophotonics* 2:021012.
- Piao HH, Rajakumar D, Kang BE, Kim EH, Baker BJ (2015) Combinatorial mutagenesis of the voltage-sensing domain enables the optical resolution of action potentials firing at 60 Hz by a genetically encoded fluorescent sensor of membrane potential. *J Neurosci* 35:372-385.
- Murata Y, Iwasaki H, Sasaki M, Inaba K, Okamura Y (2005) Phosphoinositide phosphatase activity coupled to an intrinsic voltage sensor. *Nature* 435:1239-1243.
- Lee S, Geiller T, Jung A, Nakajima R, Song YK, Baker BJ (2017) Improving a genetically encoded voltage indicator by modifying the cytoplasmic charge composition. *Sci Rep* 7:8286.
- Baker BJ, Lee H, Pieribone VA, Cohen LB, Isacoff EY, Knöpfel T, Kosmidis EK (2007) Three fluorescent protein voltage sensors exhibit low plasma membrane expression in mammalian cells. *J Neurosci Methods* 161:32-38.
- Miesenböck G, De Angelis DA, Rothman JE (1998) Visualizing secretion and synaptic transmission with pH-sensitive

- green fluorescent proteins. *Nature* 394:192-195.
15. Ng M, Roorda RD, Lima SQ, Zemelman BV, Morcillo P, Miesenböck G (2002) Transmission of olfactory information between three populations of neurons in the antennal lobe of the fly. *Neuron* 36:463-474.
 16. Li Q, Wanderling S, Paduch M, Medovoy D, Singharoy A, McGreevy R, Villalba-Galea CA, Hulse RE, Roux B, Schulten K, Kossiakoff A, Perozo E (2014) Structural mechanism of voltage-dependent gating in an isolated voltage-sensing domain. *Nat Struct Mol Biol* 21:244-252.
 17. Han Z, Jin L, Platasa J, Cohen LB, Baker BJ, Pieribone VA (2013) Fluorescent protein voltage probes derived from ArcLight that respond to membrane voltage changes with fast kinetics. *PLoS One* 8:e81295.
 18. Schneider MF, Chandler WK (1973) Voltage dependent charge movement of skeletal muscle: a possible step in excitation-contraction coupling. *Nature* 242:244-246.
 19. Armstrong CM, Bezanilla F (1973) Currents related to movement of the gating particles of the sodium channels. *Nature* 242:459-461.
 20. Keynes RD, Rojas E (1974) Kinetics and steady-state properties of the charged system controlling sodium conductance in the squid giant axon. *J Physiol* 239:393-434.
 21. Akabas MH, Stauffer DA, Xu M, Karlin A (1992) Acetylcholine receptor channel structure probed in cysteine-substitution mutants. *Science* 258:307-310.
 22. Mannuzzo LM, Moronne MM, Isacoff EY (1996) Direct physical measure of conformational rearrangement underlying potassium channel gating. *Science* 271:213-216.
 23. Kang BE, Baker BJ (2016) Pado, a fluorescent protein with proton channel activity can optically monitor membrane potential, intracellular pH, and map gap junctions. *Sci Rep* 6:23865.
 24. Treger JS, Priest MF, Bezanilla F (2015) Single-molecule fluorimetry and gating currents inspire an improved optical voltage indicator. *Elife* 4:e10482.
 25. Killian JA (1998) Hydrophobic mismatch between proteins and lipids in membranes. *Biochim Biophys Acta* 1376:401-415.
 26. Sung U, Sepehri-Rad M, Piao HH, Jin L, Hughes T, Cohen LB, Baker BJ (2015) Developing fast fluorescent protein voltage sensors by optimizing FRET interactions. *PLoS One* 10:e0141585.
 27. de Planque MR, Kruijtz JA, Liskamp RM, Marsh D, Great-house DV, Koeppe RE 2nd, de Kruijff B, Killian JA (1999) Different membrane anchoring positions of tryptophan and lysine in synthetic transmembrane alpha-helical peptides. *J Biol Chem* 274:20839-20846.
 28. Killian JA, von Heijne G (2000) How proteins adapt to a membrane-water interface. *Trends Biochem Sci* 25:429-434.
 29. Baker BJ, Mutoh H, Dimitrov D, Akemann W, Perron A, Iwamoto Y, Jin L, Cohen LB, Isacoff EY, Pieribone VA, Hughes T, Knöpfel T (2008) Genetically encoded fluorescent sensors of membrane potential. *Brain Cell Biol* 36:53-67.